Friction and the Development of Hard Alloy Surface Microstructures during Wear

S.F. Gnyusov and S.Yu. Tarassov

Investigations of wear in sliding friction of WC-Hadfield steel hard alloy against cast tool steel have been carried out in a broad range of velocities and pressure values. Structural and phase composition variations have been revealed. Friction-affected zone was found to be 450 μm in depth. Structural $\gamma \rightarrow \alpha, \gamma \rightarrow \varepsilon$ transformation regions are located within 100 μm of the surface. These transformations contributed to the total solid solution deformation hardening.

Keywords friction transformations, WC-Co, WC-Ni, wear

Introduction

A solution to the problem of durability in extrusion tools used in fabricating polymeric materials may help save labor and material resources. This is a special problem for working components in plastic material processing machines such as "cutter-die" couples working at elevated temperatures and high specific pressures.

An analysis of industrial use of dies at the Tomsk Petroleum Processing Plant (Tomsk, Russia) shows that hard alloy inserts of WC-Co and WC-Ni brazed into the die with the use of silver, brass, or cupronickel brazings do not provide long-term durability of equipment. Nonuniform wear occurs both at the working surface of the matrix and at blades of rotation cutters due to the considerable difference in hardness between hard alloy die inserts and the matrix. The results are the destruction of the brazed joint and chipping in hard alloy inserts and cutters with ensuing sticking. The situation worsens in the granulation of polymers filled with hard fillers. Embrittlement of WC-Ni, WC-Co alloys is a main drawback, especially when the polymers contain a hard component. Because dislocation slip is a basic mechanism of deformation in a binding phase, the effective stress relaxation ability of a solid-solution matrix can be obtained only in highly diluted composites. Otherwise, this mechanism does not work in small volumes of material due to the strong constraint of the binder phase and pinning of dislocations. A nonuniform stress state, which appears in a composite material under loading, may cause an appearance of stress concentrators that may initiate, in their turn, the fracture of material.

To increase the service life of a die, its working surface was armored with WC-Hadfield steel hard alloy (Fig. 1). The distinctive property of the material is that at around room temperature its binding phase is metastable austenite and during loading peak stresses can be reduced due to martensitic transformation occurring in solid-solution matrix and following redistribution of stress. This provides a twofold increase in the ultimate deformation compared to the traditional WC-Co composites, with strength being kept constant with variations in hard phase content.

S.F. Gnyusov and **S.Yu. Tarassov,** Institute for Strength Physics and Materials Sciences, 634055, Tomsk, Russia, Academicheskiy, 5, 21.

To select optimal work regimes and to elucidate the character of wear of the proposed composite, full-scale tests of a cutter-die friction couple were carried out. For this purpose an attempt was made to investigate structural and phase composition variations and to determine the wear of WC-Hadfield steel composite in friction with an as-cast cutter tool steel at various friction velocities and pressures.

Materials and Experimental Procedures

A hard alloy containing tungsten carbide and a high manganese steel (30 wt%) was studied. The binder was fully austenitic after the composite was quenched from 1100 °C in oil. Specimens were cylindrical 10 mm diam pins with 20 mm height. The counterbody was a 350 mm diam disk of cast tool steel consisting structurally of martensite, excess tungsten- and vanadium-base $M_{12}C$ carbides. Small amounts of residual austenite were also detected. This steel is used to manufacture cutters for polymer granulation.

The initial structure of the sintered-and-quenched WC-Hadfield steel hard alloy comprises WC grains (hexagonal close-packed crystal lattice having the following parameters: $a = 0.21$ nm, $c = 0.293$ nm) uniformly distributed in the iron-base γ solid solution (Fig. 2). Minor amounts (less than 1%) of $M_{12}C$ with a cubic lattice parameter of $a = 1.095$ nm are present.

Tribotechnical characteristics and wear resistance of the material were evaluated using a pin-on-disk testing proce-

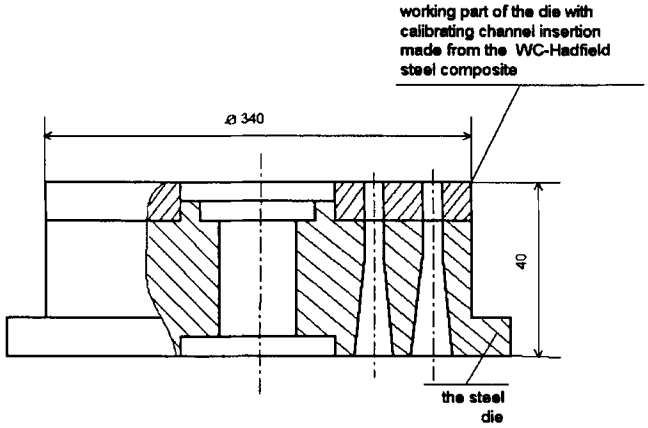

Fig. 1 Schematic of plastic material extrusion die

dure conducted on a 2168 UMT-1 friction machine (Tochpribor, Ivanovo, Russia). Specimens were loaded by a pneumatic device in 350 to 1050 N intervals. Velocity ranged from 0 to 10 m/s. The duration of each test corresponded to the length of friction path $L = 4500$ m, irrespective of the counterbody's rotation rate. Friction torque and temperature of the specimen were measured automatically. Structural investigations were carried out on specimens after the full cycle of tests included all the combinations of load and friction velocities. The total friction path length was 90,000 m.

Wear measurements were conducted with a micrometer at every combination of load and velocity values. Wear rate was evaluated by the difference between successive micrometer readings at friction path length held constant.

Microhardness of the studied specimens was measured by a PMT-3 instrument (LOMO, Sanct-Petersburg, Russia). Microstructure was investigated using an optical microscope "Neophot-21" (Carl Zeiss, Jena, Germany) and an electron transmission microscope. Thin foils were obtained by ion beam thinning of previously electroerosion-cut section. Phase composition was determined by x-ray diffractometry using filtered Cu radiation.

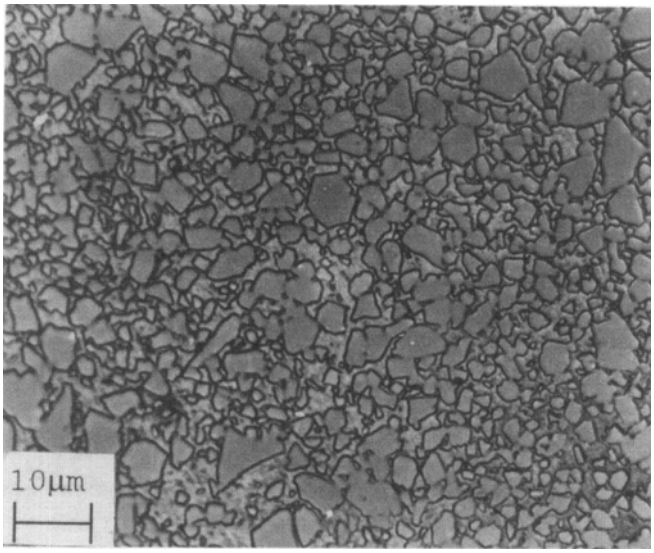

Fig. 2 Initial structure of WC-Hadfield steel composite

Results

Figure 3 shows the dependencies of the friction coefficient, wear rate, and temperature of the friction zone in relation to the normal load and slide velocity. As can be seen from Fig. 3(a), the temperature of the studied specimens is almost monotonically increased with the pressure and sliding speed except for pressure values falling within the 750 to 800 N range.

The true values of the temperature in the contact zone are much higher because a chromel-alumel thermocouple was inserted 1 mm below the friction surface. The character of friction coefficient variation with the load and slide velocity is a complex one (Fig. 3c). There is a substantial difference between its behavior at low and high velocities. The coefficient of friction grows sharply with the load at low values of slide velocity (0 to 6 m/s) and diminishes at higher values. The maximum in friction is achieved at low velocities and under heavy loading (1000 N) with ensuing fall in friction as the velocity increases. The dependence of wear on load and velocity is characterized by a region of minimum wear appearing within the 550 to 750 N loading range. This minimum exists irrespective of the sliding speed (Fig. 3b). The maximum values of wear are found to correlate with the maximum in friction at low velocities and maximum load. At a maximum load, both friction coefficient and wear tend to decrease with an increase in sliding speed.

An investigation of friction surface in relation to the different regions of the corresponding dependencies of wear and friction revealed the differences in friction and wear mechanisms.

The normal abrasive-oxidative wear grooves were observed on friction surface of pins being loaded below 800 N. The products of wear served as abrasives. The white embedded particles can also be seen on the sliding friction surface (Fig. 4a). Their

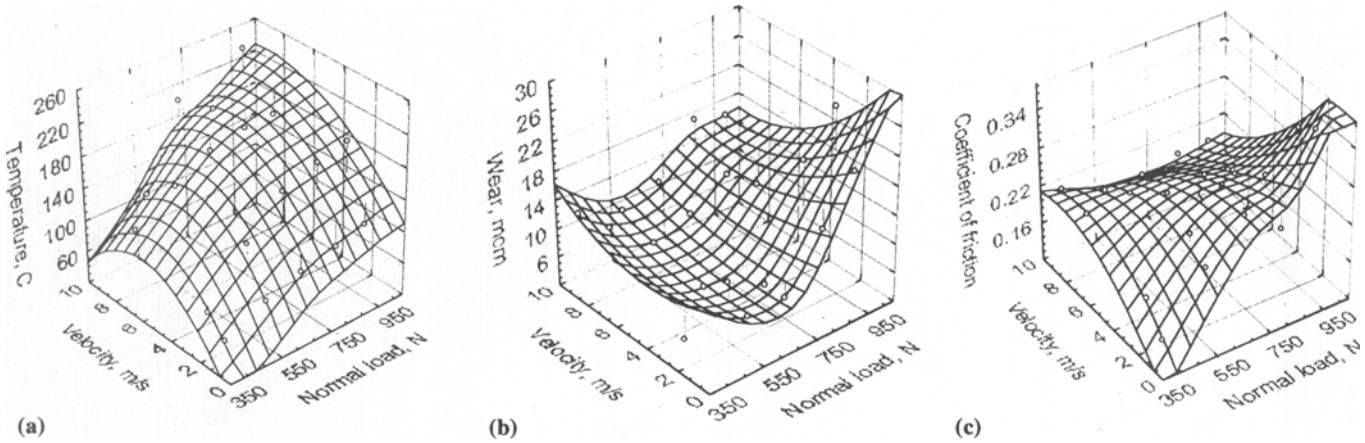

Fig. 3 The least square dependencies of friction-zone temperature (a), wear (b), and friction coefficient (c) in relation to the normal load and slide velocity

chemical composition is illustrated in Fig. 5, from which one can see that they consist mostly of iron, tungsten, and vanadium. Their diffraction pattern corresponds to that of the $M_{12}C$ carbide. The amount of these particles tends to decrease with an increase in the load and slide velocity, that is, with the temperature of the friction zone.

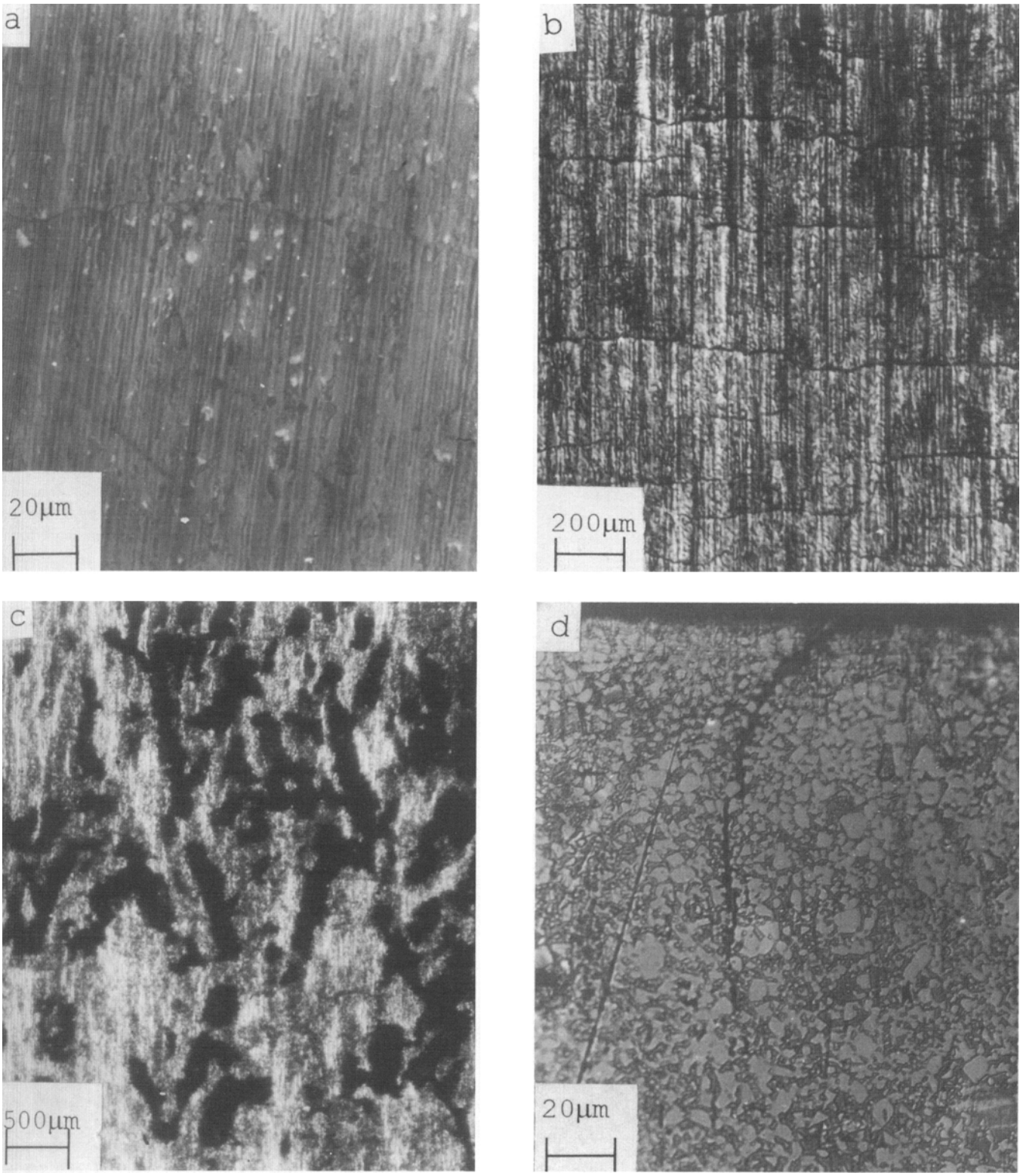

Fig. 4 Friction surface of WC-Hadfield steel composite after full cycle of tests. (a) White particles. (b) Transverse cracks. (c) Adhesive wear. (d) Cracking in friction-affected zone (cross section)

The regularly spaced transverse cracks were observed at the friction surface of the specimens tested at loads higher than 800 N (Fig. 4b). Such cracks are commonly found on the surface of various hard materials under severe friction conditions. In this case, their penetration depth was not greater than 80 to 100 μm. The fracture was transgranular and intergranular (Fig. 4d).

As the load increased, vast zones of adhesive wear became apparent (Fig. 4c).

The dependence of microhardness on the distance from the top of the specimen gives evidence that the material is considerably hardened down to the depth of 500 μm (Fig. 6).

This dependence may be arbitrarily divided into three zones: first is a zone with a constant high hardness (zone 1, 100 μm), second is a zone with the gradually decreasing hardness (zone 2, 400 μm), and finally zone 3 has the initial value of microhardness.

Four phases were found by x-ray diffraction at the surfaces of the specimens after the tests: WC, Fe_3O_4, FeO, and $M_{12}C$. No sign of the initial γ phase was detected on the very surface of the specimens.

A layer-by-layer x-ray analysis showed that both ε and α phases are present in the subsurface 10 μm thick layer together with the initial γ solid solution (Fig. 7). The amounts of phases were evaluated by the intensity of (002)ε, (110)α, and (111)γ diffraction peaks in relation to the intensity of WC (101).

As is apparent from Fig. 7, the ε phase is concentrated in a thin 5 μm thick layer, whereas the α phase is detected down to 100 μm in depth. The structure of the friction-affected zone is presented in Fig. 8. One can see that much of the binder is the α phase (dark zones). Transmission electron microscopy dark field image of the worn surface layer structure of the composite together with the corresponding microdiffraction pattern is shown in Fig. 9. The microdiffraction pattern is identical to that of Fe_3O_4, and the micrograph was obtained by setting the selector diaphragm on the (220) and (311) rings. The size of oxide particles gives evidence that the intense process of fragmentation occurred on the surface of the hard alloy. The fragmentation in friction is a common feature of the worn surface structure in different materials, and hard alloys are not the exception.

Figure 5 gives a chemical composition of the initial material surface layers compared to that of surface layers after friction (1000 N, 10 m/s). The depletion in manganese and tungsten together with simultaneous enrichment in chromium, iron, nickel, and vanadium are the characteristics of friction under the above conditions.

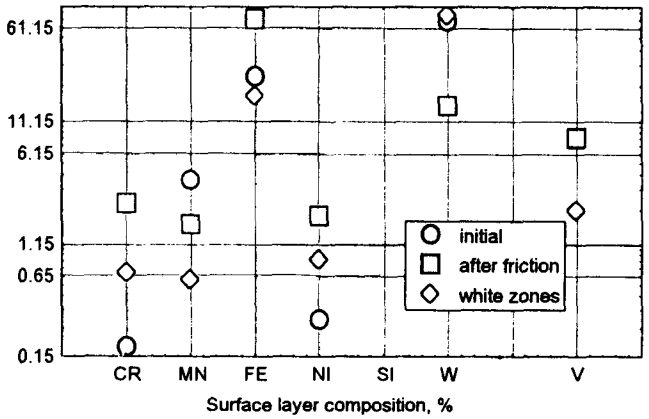

Fig. 5 Chemical composition of WC-Hadfield steel surface layers before and after the tests

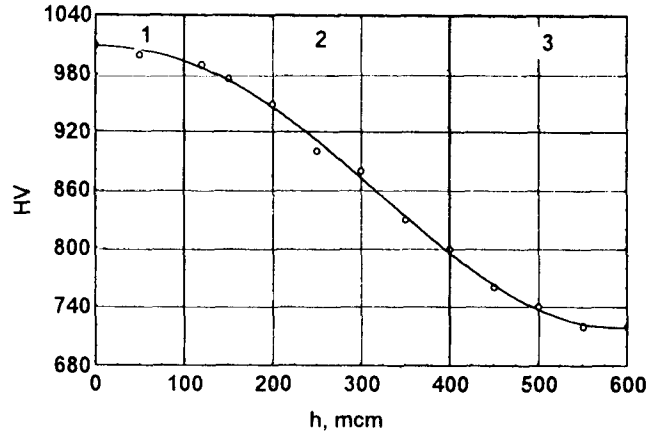

Fig. 6 Hardening of subsurface layers. Hardness as a function of distance away from the sliding surface

Discussion

The shapes of dependencies in Fig. 3 suggest to the authors that a complex process of structural changes takes place in the surface layers of the material under the mutual action of deformation and temperature. Great amounts of white layers are present on the surface of the specimens after the friction tests are carried out at low values of load and velocity. This is evidence that so-called secondary structures based on wear products are formed. The structural γ → ε transformation that occurs during the severe deformation of surface layers may decrease friction and wear at low values of velocity and load. Wear and friction at the beginning of the diagram in Fig. 3(b) and (c) are defined by the interaction between hard alloy particles and the disk material. The binding phase is not hardened enough to stabilize the friction and wear coefficients. Having been stabilized at higher values of load and velocity by the formation of the secondary structures (white zones), the friction coefficient is kept approximately constant elsewhere except for high loads. The decrease in wear and friction at 550 to 750 N is due to γ → ε martensitic transformation in the subsurface layers of a composite and formation of the secondary structures (white zones) from tungsten carbide wear debris and material of the disk.

With the increase in the load and velocity, the rising temperature must initiate ε → γ transformation mechanism, but the higher the temperature is the more intense is the oxidation. The oxide films help stabilize friction and wear at heavy loading (1000 N, 10 m/s), even in the absence of a γ → ε stress relaxation mechanism. However, the intense loading may lead to the formation of the ε phase in a thin layer even under severe friction with specimen volume temperature of 240 °C (Fig. 7).

High temperatures of friction together with the disk/pin transfer of the material provide a dramatic change in the chemi-

cal composition of the surface layers. The most important fact is the decrease in manganese content that will facilitate $\gamma \rightarrow \alpha$ transformation within the 100 μm layer. Precipitation of carbides from the solid solution is another type of structural evolution at elevated temperatures. The disk/pin transfer of the material is responsible for the friction surface layer being enriched with vanadium, iron, nickel, and chromium. On cooling, this layer—mechanically alloyed by the metal of a disk—demonstrates high values of microhardness (1000 HV).

The substructural hardening of the solid solution is the reason for raised value of microhardness at 100 to 500 μm depth (Fig. 6).

Judging by the results of an x-ray layer-by-layer analysis, the initial γ phase is not detected on the very surface of the specimens and appears only after the removal of 5 μm deep layer of the material. This depth approximately corresponds to the depth of x-ray penetration into the material. There are two reasons that may explain the absence of the γ phase on the sliding surface. It may be defined, on the one hand by the considerable differences in hardness between the structural constituents of the composite, which may lead to more intense wear and removal of a binding phase. As a result, the surface is enriched with hard WC fragments that indent the matrix being partly involved in friction as wear products.

On the other hand, growth of the contact zone temperature together with the simultaneous action of the environment results in formation of a thin oxide film (several microns thick) that shields the γ phase matrix in x-ray studies. The surface layer of the specimens suffered intense oxidation, as shown in Fig. 9.

The white zones found at the friction surface of a hard alloy are the complex carbides of the $M_{12}C$ type. These zones are most likely formed by virtue of pin/disk material transfer and accumulation of wear products in friction. The phase transformations occurring in the surface layers may add to the process. Friction and wear can be stabilized by the existence of these zones while the mutual loading and speed factor is kept below their bearing ability.

Cracking at loads higher than 800 N can be related to the thermal fracture (Ref 1) occurring in brittle materials with poor heat conductivity. Hard alloys are this type of material. However, the use of structurally unstable binding phase facilitates the relaxation of external stresses (up to a definite limit) due to

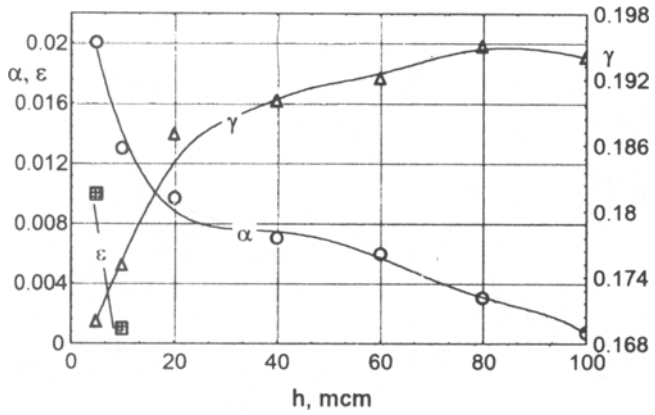

Fig. 7 Phase composition of the friction-affected zone in WC-Hadfield steel composite

phase transformations ($\gamma \rightarrow \alpha$, 10 to 12% of α phase; $\gamma \rightarrow \varepsilon$, 6 to 8% of ε phase), solid-solution hardening, and redistribution of stresses from the matrix to the carbide particles. As a result, the mutual deformation of a binding phase and carbide particles takes place. Further increase in the load may lead to the cracking and ensuing detachment of large particles by adhesion.

Another reason for the transverse periodic cracking may be that cracks are initiated by friction force autooscillations arising in adhesion wear due to falling sliding speed dependence of the friction coefficient (Fig. 3c) (800 N, 8 m/s) (Ref 2).

Conclusions

- The WC-Hadfield steel composites are hardened in friction by at least three mechanisms: martensitic $\gamma \rightarrow \varepsilon$ transfor-

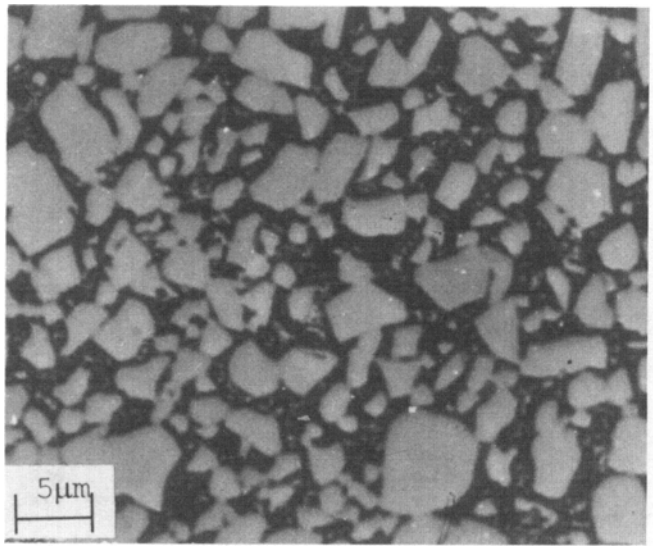

Fig. 8 The structure of the friction-affected zone

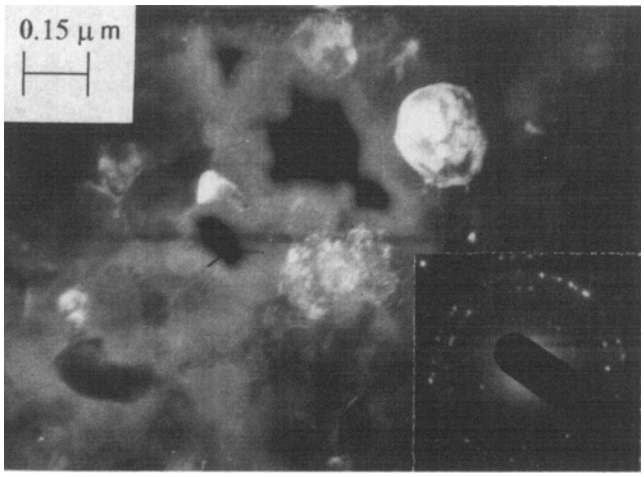

Fig. 9 TEM dark field image and microdiffraction pattern of surface layer structure in WC-Hadfield steel composite after severe friction

mation, $\gamma \rightarrow \alpha$ transformation, and substructural solid-solution hardening.

- Transformation-induced gradient of mechanical properties enables more uniform wear of the composite in friction with tool steel, especially at high sliding speed; the deformation-induced $\gamma \rightarrow \varepsilon$ transformation occurs in thin subsurface layers over the entire range of load and sliding speed values including the maximum temperatures reached in the experiment.
- The most destructive friction regime is a combination of low velocity with high load.

References

1. D.N. Garkunov, *Mashinostroenie*, Tribotehnika, 1989, 389 pages (in Russian)
2. V.L. Popov and A.V. Kolubaev, Generatsia Poveruhnostnyh Voln pri Vneshnem Trenii Uprugih Tverdyh Tel, *Zh. Tek. Phys.*, Vol 19, 1995, p 91-94 (in Russian)